Demonstration of a Tunable Microwave-Photonic Notch Filter Using Low-Loss Silicon Ring Resonators

Demonstration of a Tunable Microwave-Photonic Notch Filter Using Low-Loss Silicon Ring Resonators

Mahmoud S. Rasras, *Member, IEEE*, Kun-Yii Tu, *Member, IEEE*, Douglas M. Gill, Young-Kai Chen, *Fellow, IEEE*, Alice E. White, *Senior Member, IEEE*, Sanjay S. Patel, Andrew Pomerene, *Associate Member, IEEE*, Daniel Carothers, James Beattie, Mark Beals, *Member, IEEE*, Jurgen Michel, *Member, IEEE*, and Lionel C. Kimerling, *Member, IEEE*

***Abstract*—We present a fully tunable multistage narrowband optical pole-zero notch filter that is fabricated in a silicon complementary metal oxide semiconductor (CMOS) foundry. The filter allows for the reconfigurable and independent tuning of the center frequency, null depth, and bandwidth for one or more notches simultaneously. It is constructed using a Mach–Zehnder interferometer (MZI) with cascaded tunable all-pass filter (APF) ring resonators in its arms. Measured filter nulling response exhibits ultranarrow notch 3 dB BW of 0.6350 GHz, and nulling depth of 33 dB. This filter is compact and integrated in an area of 1.75 mm^2. Using this device, a novel method to cancel undesired bands of 3 dB bandwidth of $<$ 910 MHz in microwave-photonic systems is demonstrated. The ultranarrow filter response properties have been realized based on our developed low-propagation loss silicon channel waveguide and tunable ring-resonator designs. Experimentally, they yielded a loss of 0.25 dB/cm and 0.18 dB/round trip, respectively.**

***Index Terms*—Integrated optics, microwave-photonics, notch filter, optical waveguide components.**

I. Introduction

RECENTLY, there has been a major progress in the development of complementary metal oxide semiconductor (CMOS) silicon-based photonic components. Integrating photonic components in a CMOS platform provides the benefits of a significant reduction in cost and size. In addition, there is great potential in creating new functions from incorporating photonics and electronics on the same silicon chip [1]. Optical filters are a key enabler of this technology, among which, notch filters can play a critical role in photonic and microwave-photonic systems to enable the blocking of undesired spectral content [2], signal monitoring, or subcarrier processing [3].

In this paper, we present a compact ultranarrow bandwidth optical notch filter that has a 3 dB bandwidth of 625 MHz at 1.55 μm. The filter is fabricated entirely in a commercial CMOS foundry using silicon channel waveguides. It is designed based on a pole-zero architecture [3] where it is constructed using Mach–Zehnder with multistage all-pass ring-resonator filters in its arms. Additionally, we demonstrate the potential use of this device in a microwave-photonic system to block undesired narrow radio-frequency (RF) bands of 3 dB bandwidth of 910 MHz over an ultrabroad tuning range. As high-propagation loss in silicon waveguides may hinder realizing a high-optical component performance, we will also discuss design methods that substantially reduce the propagation loss in our waveguides.

This paper is organized as follows. The filter design and optimization are described in Section II. This section also discusses the impact of waveguide loss on the filter performance. Techniques to reduce optical losses in our ring resonators, which are critical building blocks of this device are presented in Section III. Experimental results demonstrating the filter's optical response and its employment in microwave-photonic systems are described in Sections IV. Finally, a summary is presented in Section V.

II. Filter Design

A narrow notch filter response can be realized using a Mach–Zehnder interferometer with a delay in one of its arms. Though this device is simple, it has a limited degree of tunability and tradeoffs between the filter free spectral range (FSR), nulling depth, and nulling bandwidth [6]. Alternatively, one could use an all-pole ring resonator [5]. This filter allows for a narrowband notch filter response and tuning of frequency notch position. However, it requires balancing the resonator coupling and its optical round-trip loss (RTL) to obtain a deep notch response. In this paper, we use a pole-zero filter constructed using a Mach–Zehnder interferometer (MZI) with cascaded tunable all-pass filter (APF) ring resonators in one of its arms [3], [4]. The filter allows for the independent tuning of the center frequency, bandwidth and null depth, for one or more notches simultaneously. A schematic diagram illustrating our filter layout and an image of the chip is shown in Fig. 1. In this implementation, a notch in the frequency response occurs at the resonance positions of the APFs. The filter's response

Manuscript received June 13, 2008; revised September 28, 2008. First published April 21, 2009; current version published June 24, 2009. This work was funded by the government Defense Advanced Research Projects Agency (DARPA) project EPIC, supervised by Dr. J. Shah. The program is executed by the Microsystems Technology Office (MTO) under Contract HR0011-05-C-0027.

M. S. Rasras, K. Y. Tu, D. M. Gill, Y. K. Chen, A. E. White, and S. S. Patel are with Alcatel-Lucent, Bell Laboratories, Murray Hill, NJ 07974 USA (e-mail: rasras@alcatel-lucent.com; kunyiitu@alcatel-lucent.com; dmgill@alcatel-lucent.com; ykchen@alcatel-lucent.com; aew@alcatel-lucent.com; e-mail: sanjay@alcatel-lucent.com).

A. Pomerene, D. Carothers, and J. Beattie are with BAE Systems, Nashua, NH 03061-0868 USA (e-mail: andrew.pomerene@baesystems.com; daniel.carothers@baesystems.com; james.beattie@baesystems.com).

M. Beals, J. Michel, and L. C. Kimerling are with the Massachusetts Institute of Technology, Cambridge, MA 02139 USA (e-mail: mbeals@mit.edu; jmichel@mit.edu; lckim@mit.edu).

Color versions of one or more of the figures in this paper are available online at http://ieeexplore.ieee.org.

Digital Object Identifier 10.1109/JLT.2008.2007748

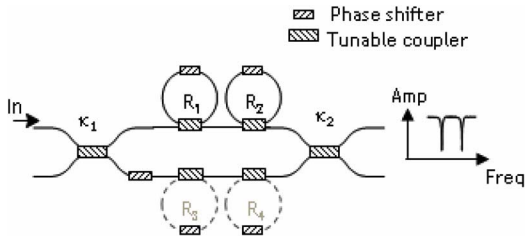

Fig. 1. A fourth-order pole-zero filter can be used as a nulling filter by turning ON/OFF certain resonators in the device.

is determined by the APF's and MZI input/output-coupling coefficients. Note that in this layout either the upper or lower APFs in each MZI arm can be used, while the rings on the opposite arm are turned OFF by using a tunable MZI coupler embedded in the ring design.

A. Frequency Response

The notch filter bandwidth and nulling depth are determined by MZ-coupling coefficients (κ_1 and κ_2) and by the amount of the frequency-dependent nonlinear phase shifts introduced by the ring resonators into its arm. This nonlinear phase shift generates a group delay difference between the MZ arms, the amount of which is controlled by ring-coupling ratios [4]. This group delay difference produces nulls in the filter response at the resonance frequency locations of the APF rings. The notch filter response described using the z-transformation representation can be written as

$$\begin{bmatrix} H_{\mathrm{T}}(z) \\ H_C(z) \end{bmatrix} = \begin{bmatrix} c_2 & -js_2 \\ -js_2 & c_2 \end{bmatrix} \begin{bmatrix} H_{\mathrm{R}}(z) & 0 \\ 0 & e^{-\mathrm{j}\beta} \end{bmatrix} \times \begin{bmatrix} c_1 & -js_1 \\ -js_1 & c_1 \end{bmatrix} \quad (1)$$

where H_{T} and H_{c} are the through and cross-ports filter response, respectively. $z^{-1} = e^{-j2\pi fT}$, f is the optical frequency, T is the ring unit delay length. $c_1 = \sqrt{1-k_1}, c_2 = \sqrt{1-k_2}, s_1 = \sqrt{k_1}$, and $s_2 = \sqrt{k_2}$, and k_1, k_2 are the coupling ratios of the first and second tunable couplers of the MZ, respectively. $j = \sqrt{-1}$, and β is a phase factor introduced to balance the phase in the MZ arms. The function H_{R} is the frequency response of the cascaded all-pass ring-resonator filter which is given by

$$H_{\mathrm{R}}(z) = \prod_{r}^{N} \left[\frac{e^{-j\varphi_r}(\rho_r e^{+j\varphi_r} - \gamma z^{-1})}{1 - \rho_r e^{-j\varphi_r}\gamma z^{-1}} \right] \quad (2)$$

where N is the number of rings, $\rho_r = \sqrt{1-\kappa_r}$ where K_r is the ring-coupling ratio. Each ring will introduce a notch at its resonance frequency. The ring's RTL is given by $-20*\log_{10}(\gamma)$, and φ_r is the ring's phase. The unit delay can then be calculated from the ring parameters which is defined as $T = (L/c_0)n_{\mathrm{g}}$, where L is the ring-round-trip length, c_0 is the speed of light in the vacuum, and n_{g} is the silicon waveguide group index.

In this design, to obtain a high-notch depth, the MZ-coupling coefficients are adjusted to balance the losses introduced by the ring resonator. Fig. 2 shows an example of the notch response calculated for different nulling bandwidths. In this figure, the notch depth is kept constant, while the 3 dB bandwidth is varied

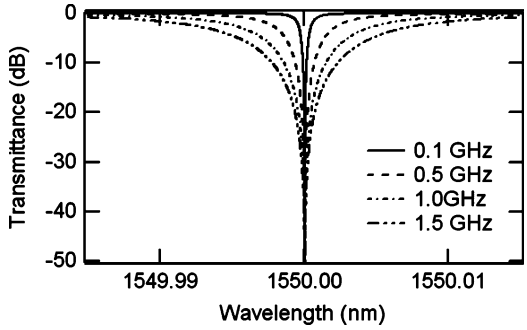

Fig. 2. Calculated notch filter response for different bandwidths performed at a constant notch depth.

TABLE I
CALCULATED FILTER-COUPLING COEFFICIENTS ASSUMING A RING NOTCH DEPTH OF −30 DB. (A) LOSSLESS CASE, (B) APF ROUND TRIP LOSS OF 0.15 DB

a) Round trip loss =0.0dB			
BW (GHz)	K1	K2	ρ
0.5	0.5379	0.5064	0.9647
1	0.5532	0.5217	0.9306
1.5	0.5653	0.5341	0.8972
b) Round trip loss =0.15dB			
0.5	0.3542	0.9318	0.9773
1.0	0.3542	0.6282	0.9468
1.5	0.4301	0.5826	0.9131

between 0.1 GHz and 1.5 GHz. These curves are calculated for a lossless APF case. Nonlinear optimization techniques using commercially available Matlab software are used to determine the filter coefficients. The optimization process takes into account the APF round-trip loss. Table I illustrates two design examples for a filter set at the notch depth of −30 dB for bandwidths ranging from 0.5 to 1.5 dB. The coefficients are calculated assuming rings with RTL of 0 dB and 0.15 dB. It is clear from this table that for rings with loss, more light is coupled in the MZ arm where the ring is placed (see Table I(b), 2nd column) and the opposite is happening to MZ second coupler (K2). Additionally, for a narrower notch, light should be less coupled to the APF. Note that, as discussed previously, the notch occurs due to the induced nonlinear phase generated in one of the MZ arms by the APF. Therefore, the MZ-coupling ratios are adjusted to compensate for the loss generated by the ring resonator.

III. IMPACT OF RING-ROUND-TRIP LOSS & DESIGN OPTIMIZATION

The RTL of the resonators affects the notch bandwidth and depth by limiting the ability to realize narrow notch bandwidths while at the same time maintains a deep null response. The impact of the ring's RTL on the minimal achievable bandwidth is illustrated in Fig. 3 calculated for a filter with an FSR of 43 GHz

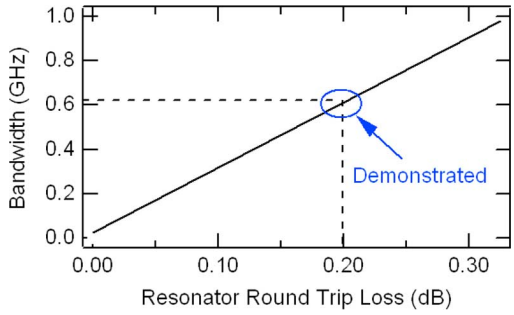

Fig. 3. Impact of the ring's RTL on narrowest achievable notch bandwidth calculated at a 3 dB bandwidth for a 35 dB null depth and at FSR of 43 GHz.

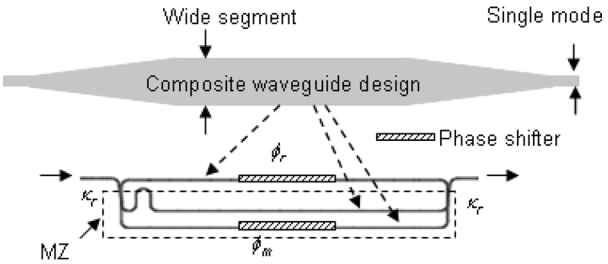

Fig. 4. Schematic diagram of the ring-resonator layout. Loss is reduced by maximizing the lengths of wide waveguide inside the ring's tunable couplers and feedback path.

and a null depth of -35 dB. As shown in this figure, increased ring-resonator RTL linearly degrades the narrowest achievable bandwidth, limiting the performance of the filter.

Loss in the silicon ring resonator is attributed mainly to waveguide propagation loss, bend loss, and substrate leakage. The last two loss mechanisms can be substantially reduced by using sufficiently large bend radius waveguides and by employing thick lower cladding layer (1.5 μm–3 μm) to prevent the waveguide evanescent field from coupling to the substrate, respectively. Propagation loss in silicon waveguides, however, is dominated by scattering from the waveguide sidewalls. Sparacin *et al.* have shown that this loss mechanism can be reduced by sidewall smoothing processes using wet chemical oxidation [5]. Additionally, they have shown that the loss can be reduced by widening the waveguide width; see also [5]. To reduce the RTL in our tunable-ring resonators, the design is implemented to maximize the portion of wide waveguide in the layout. Details of the ring's design are shown in Fig. 4. It is constructed using a tunable MZ coupler and a feedback path connecting the output of the MZ coupler to one of its inputs. In this layout, the feedback path and the MZ arms are designed using wide straight waveguide segments. A transition to the straight portion of the waveguide is performed by an adiabatic taper. The taper begins after the bent portion ends, as long as the length of the straight section of the waveguide is long enough to accommodate the taper. Additionally, we also incorporated a tapering of the waveguide width into the bent portion of the waveguide. The width of the bent segment is varied smoothly to a lateral width at which only the fundamental mode propagates. This configuration advantageously increases the length of straight waveguide having the larger width and lowers loss.

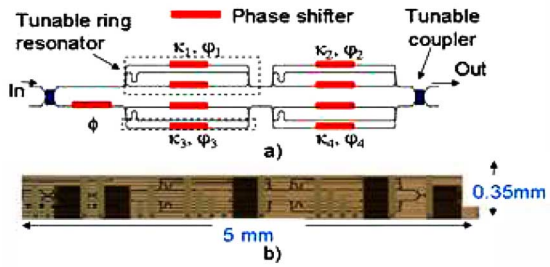

Fig. 5. (a) Design layout of a fourth-order pole-zero filter is used as a notch filter by turning ON/OFF certain resonators in the device. (b) Image of the chip.

IV. Measured Filter Response

A. Fabrication

Silicon on insulator (SOI) wafers with a lower cladding oxide thickness of 3 μm and the buried channel waveguide core thickness of 0.2 μm are used to implement this filter. We used a deep ultraviolet (DUV) lithography (248 nm) to define our silicon waveguides. The device was entirely fabricated at BAE Systems CMOS foundry demonstrating a high level of compatibility with CMOS processing. Throughout the device, we used a small bend radius of 7 μm permitting only the TE optical polarization to propagate. Although this filter was designed to be monolithically integrated between a modulator and detector to make an optical RF channelizer, polarization diverse schemes can be implemented in a relatively straightforward way. The high-index contrast of silicon waveguides allowed the filter to be integrated in a very compact area of 5.0 mm $\times$ 0.35 mm (1.8 mm^2). A schematic of the filter design and an image of the filter chip are shown in Fig. 5(a) and 5(b), respectively.

We also employed tapered mode converters to couple light from a standard single-mode fiber (SSMF) to the silicon-buried channel waveguide. We measured a coupling loss of $\sim$4.5 dB/facet. This loss can be further reduced to less than 1 dB/facet when lensed fibers are used [8]. To tune the filter, thermo-optic phase shifters were utilized to set the coupling ratios, phases of the APFs, and the Mach–Zehnder input/output couplers. These thermo-optic heaters were processed using standard CMOS metallization processing [4]. An average power consumption of 160 mW is needed to tune this filter in different configurations. While the thermo-optic phase shifters can be tuned in milliseconds, subnanosecond tuning speeds should be achievable using technology currently being explored for the high-speed modulators such as carrier injection or carrier depletion in a reversed biased junction [9], [10].

B. Measured Waveguide Loss

To determine the optimal silicon waveguide width (w_f), we used race-track ring resonators to measure the propagation loss in our waveguides as a function of the waveguide width. In these rings, straight waveguide segments are imbedded into their circumference. The width of these segments is kept constant at *wf* while their length is increased from 0.4 mm to 4 mm across three rings, see Fig. 6(a). All other ring parameters, such as the coupling ratio, tapers length, and type of bends are kept the same. The straight waveguide loss is then extracted by linearly fitting

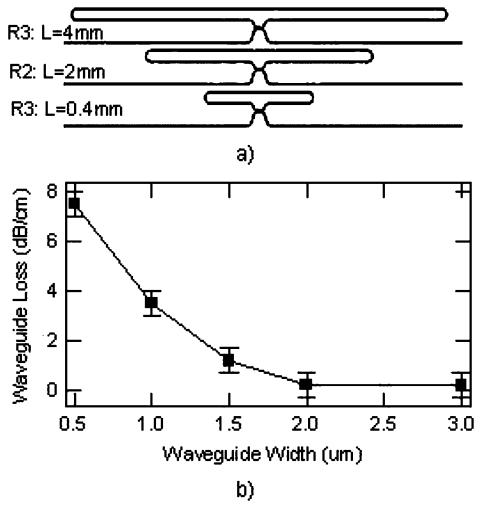

Fig. 6. (a) Schematic of race-track rings used to measure the waveguide loss. The rings have the same layout but differ in the length of straight-imbedded waveguide segments. (b) Measured loss for different straight waveguide widths. Wider waveguides showed a propagation loss as low as 0.25 dB/cm.

the measured RTL against the waveguide segment lengths. The slope of the line defines the loss per unit length. In this experiment, the RTL is extracted from the resonance response of the ring (see (2)). Fig. 6(b) shows the measured propagation loss values plotted as a function of the waveguide width. A nearly exponentially decrease in the propagation loss is observed as the waveguide gets wider. We also measured an ultralow loss waveguide of ~ 0.25 dB/cm for widths greater than 2 μm.

C. Optical Notch Filter Response

The measured notch filter response normalized to an adjacent straight waveguide loss is illustrated in Fig. 7. In this device, the fiber-to-fiber insertion loss is ~ 12 dB for the TE polarization. This loss is dominated by the coupling loss to the fiber and the propagation loss of the narrow waveguides used to connect the various components of the device. The corresponding notch response of the filter obtained using this ring is shown in Fig. 7(a) (the solid line). The filter has an FSR of 43 GHz. We measured a narrow 3 dB bandwidth of 625 MHz with a nulling depth of -33 dB realized by adjusting the resonance response of the ring and the coupling ratios of the MZI. This experimental data are in good agreement with theoretical calculations (dotted line) based on our independently measured ring RTL of 0.18 dB and is consistent with the predicted performance in Fig. 3.

By employing additional tuning rings in the multistage filter, it is possible to simultaneously null multiple frequencies at the same time. Fig. 7(b) shows a second ring tuned to produce a notch at an intermediate nulling depth. In this case, the APFs and the MZI are configured to produce a notch of 2 GHz at 3 dB bandwidth. By tuning the ring-resonance frequency, the second notch is now moved to a frequency closer to the first one, Fig. 7(c). Note that the location of the first notch is kept fixed at a wavelength of 1.55 μm ($f_c = 193.414$ THz). The above data show that this type of notch filter provides great flexibility in tuning the notch shape, frequency, and number of notches by adding more ring resonators to the device. It also provides a wide range of tunability over the entire FSR of the device.

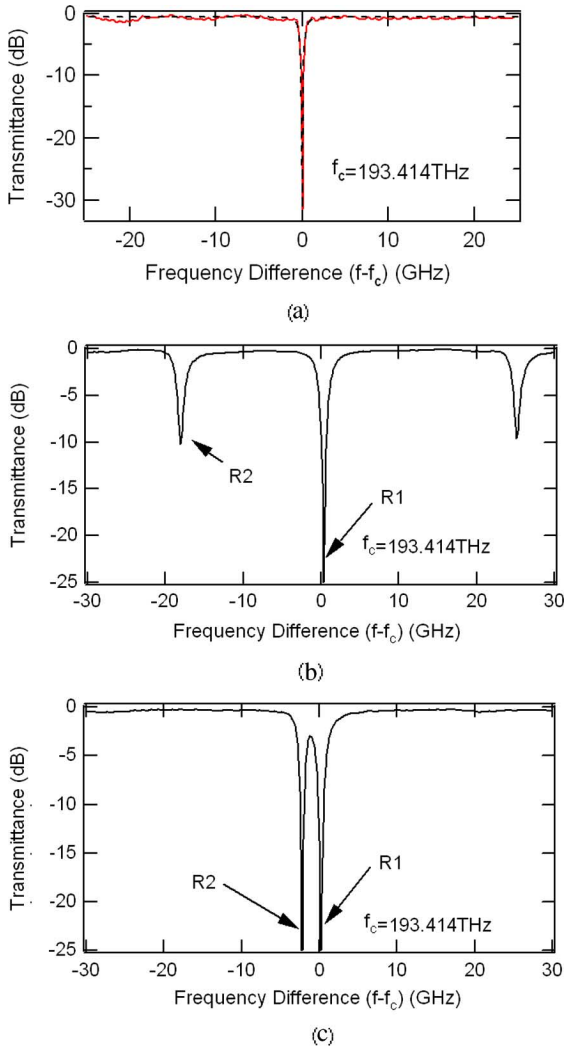

Fig. 7. Measured filter frequency response. (a) Single notch: the dashed curve is the simulated performance with a single-tuning ring and the solid line is measured data. (b) One notch is held fixed (at $f_c = 193.414$ THz, $\lambda_c = 1.55$ μm) while another notch is independently tuned using the same filter. Here, the ring is tuned to produce a notch at an intermediate nulling depth. (c) By tuning the ring-resonance frequency, the second notch is now moved to a frequency closer to the first notch.

D. Tunable Microwave-Photonic Notch Filter

Processing radio frequency (RF) signals in the optical domain has the advantage of using photonics large bandwidth and reconfigurability. In addition, this approach has less susceptiblity to electromagnetic interference [3]. High-quality optical notch and bandpass filters have been previously demonstrated using Bragg gratings, differential fiber-delays, and high-birefringence fiber-based optical components [6], [11]–[14]. However, these devices are bulky and not flexible to tune. Furthermore, in the case of differential fiber delay notch filters, a tradeoff between the filter's 3 dB bandwidth and its FSR is needed. An integrated pole-zero optical notch filter in CMOS silicon is a promising approach since it allows for significant reduction in cost and size, and enables reconfigurable filter operation. In this section, we employed our optical filter to realize a tunable microwave-photonic RF notch filter. To demonstrate this capability the setup shown in Fig. 8(a) was implemented. A narrow

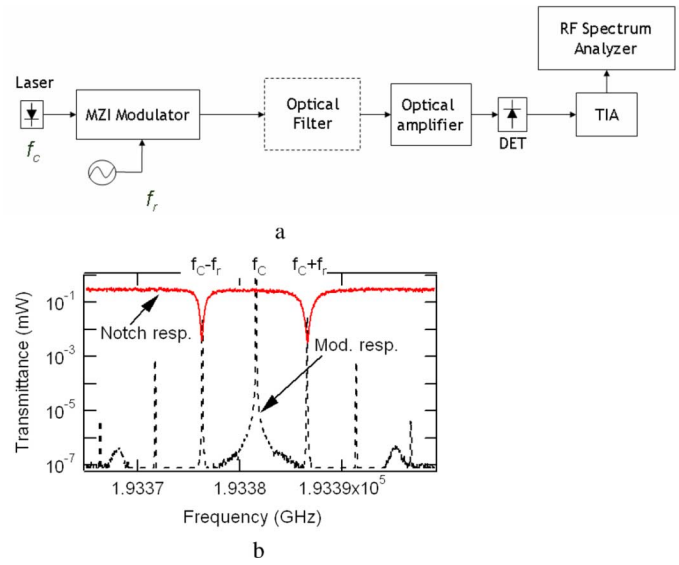

Fig. 8. (a) Block diagram of the microwave-photonic notch filter measurement setup. (b) Two notch frequencies are aligned to cancel the first-order tones generated by the MZI modulator.

linewidth CW laser and a standard (as opposed to single-sideband (SSB)) Mach–Zehnder Interferometer (MZI) $LiNbO_3$ dual-drive modulator were used to convert the RF input signal to the optical domain. At the filter output, an optical amplifier, detector (DET) and a trans-impedance amplifier (TIA) were used to convert the optical notch filter response back to the RF domain. To demonstrate the nulling of a double-sideband-modulated signal, the optical spectrum at the filter input, modulated with multiple higher order optical tones, was aligned with the two optical notches as shown in Fig. 8(b). Within the normal linear operation range of a typical electro-optic modulator, we only need to cancel the two first-order sidebands generated by the modulator. For this purpose, the nulls of two cascaded ring resonators are aligned symmetrically at the frequency positions of these two tones. This implementation avoids being restricted by a limited sideband rejection of SSB modulators. However, accurate alignment of the ring responses with that of the sidebands is important to obtain a deep and symmetric RF notch response. Therefore, in our setup, we mounted the filter on a temperature-controlled copper block which allowed controlling the notch position to within 25 MHz [4].

In our experiment, the setup is configured to generate RF nulls at various frequency positions ranging from 2 GHz to 15 GHz (range limited by our RF synthesizer and TIA). Fig. 9 shows the measured system down-converted RF response. Narrow and deep nulls, tunable over a broad range of RF frequencies, have been demonstrated. These curves were calibrated against the RF response of the system measured with all optical notches turned off. The average measured RF 3 dB bandwidth is 910 MHz with null depths better than 30 dB. A slight asymmetry in the RF notch response has been observed which could be due to a difference in the characteristics of the optical notches generated by the rings. These results demonstrate the dynamic nature of this microwave-photonic notch filter. They also show the ability to

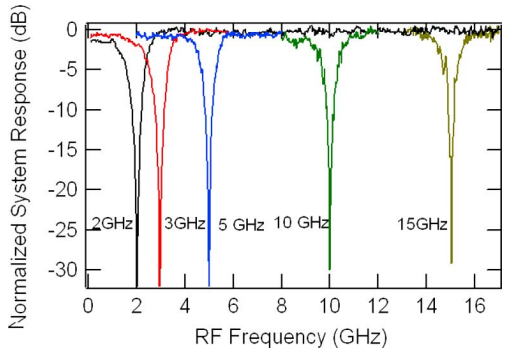

Fig. 9. Measured RF notch responses tuned at a wade range of frequencies from 2 GHz to 15 GHz.

place the notch response at any frequency to eliminate undesired spectral content.

V. Summary

We have demonstrated a fully tunable CMOS microwave-photonics notch filter with a 3 dB optical bandwidth as narrow as 635 MHz fabricated in a commercial CMOS line (910 MHz in RF domain). This narrow filter's response is realized via our developed design approaches for minimizing the round-trip-propagation loss in our ring resonators. We have also demonstrated notch depths better than 30 dB with an optical tuning range of 43 GHz (RF tuning range $>$ 15 GHz). RF measurements are limited by the bandwidth of the modulator and RF synthesizer. The dynamic nature of the filter can be potentially used for optical monitoring or to cancel undesired RF bands in microwave-photonic systems while simultaneously maintaining a frequency agile communications link.

References

[1] R. A. Soref, "Silicon-based optoelectronics," *Proc. IEEE*, vol. 81, pp. 1687–1706, 1993.

[2] J. Capmany and D. Pastor, "A tutorial on microwave photonic filters," *J. Lightw. Technol.*, vol. 24, no. 1, pp. 201–229, 2006.

[3] C. K. Madsen, M. Cappuzzo, E. Chen, L. Gomez, A. Griffin, E. J. Laskowski, L. Stulz, and A. Wong-Foy, "A tunable ultra-narrowband filter for subcarrier processing and optical monitoring," in *Proc. Opt. Fiber Commun.*, 2004, pp. 431–438, Paper Tul5.

[4] M. S. Rasras, D. M. Gill, S. S. Patel, K.-Y. Tu, Y.-K. Chen, A. E. White, A. T. Pomerene, D. N. Carothers, M. J. Grove, D. K. Sparacin, J. Michel, M. A. Beals, and L. C. Kimerling, "Demonstration of a fourth-order pole-zero optical filter integrated using CMOS processes," *J. Lightw. Technol.*, vol. 25, no. 1, pp. 87–92, 2007.

[5] D. K. Sparacin, S. J. Spector, and L. C. Kimerling, "Silicon waveguide sidewall smoothing by wet chemical oxidation," *J. Lightw. Technol.*, vol. 23, pp. 2455–2461, 2005.

[6] Y. Yin, X. Che, J. H. Wang, and K. Zheng, "Optical-fiber notch filter for storage ring transverse feedback system," in *Proc. PAC'07, T03*, 2007, pp. 4075–4077.

[7] P. Dumon, W. Bogaerts, V. Wiaux, J. Wouters, S. Beckx, J. Van Campenhout, D. Taillaert, B. Luyssaert, P. Bienstman, D. Van Thourhout, and R. Baets, "Low-loss SOI photonic wires and ring resonators fabricates with deep UV lithography," *IEEE Photon. Technol. Lett.*, vol. 16, no. 5, pp. 1328–1330, May 2004.

[8] V. Almeida, R. Panepucci, and M. Lipson, "Nanotaper for compact mode conversion," *Opt. Lett.*, vol. 28, pp. 1302–1304, 2003.

[9] C. A. Barrios, V. R. Almeida, R. Panepucci, and M. Lipson, "Electrooptic modulation of silicon-on-insulator submicrometer-size waveguide devices," *J. Lightw. Technol.*, vol. 21, pp. 2332–2339, 2003.

[10] D. M. Gill, M. Rasras, K.-Y. Tu, Y.-K. Chen, A. E. White, S. S. Patel, D. Carothers, A. Pomerene, R. Kamocsai, J. Beattie, A. Kopa, A. Apsel, M. Beals, J. Mitchel, J. Liu, and L. C. Kimerling, "Optical modulation techniques for analog signal processing and CMOS compatible electrooptic modulation," in *Silicon Photonics III, Proceedings of SPIE vol. 6898*, J. A. Kubby and G. T. Reed, Eds. Bellingham, WA: SPIE, 2008, pp. 689803–689803-11 .

[11] E. H. W. Chan, K. E. Alameh, and R. A. Minasian, "Photonic bandpass filters with high skirt selectivity and stopband attenuation," *J. Lightw. Technol.*, vol. 20, no. 10, pp. 1962–1967, 2002.

[12] E. H. W. Chan and R. A. Minasian, "Coherence-free photonic notch filter," *Elect. Lett.*, vol. 40, no. 21, pp. 1375–1377, Oct. 2004.

[13] J. X. Chen, Y. Wu, J. Hodiak, and P. K. L. Yu, "A novel digitally tunable microwave-photonic notch filter using differential group-delay module," *IEEE Photon. Technol. Lett.*, vol. 15, no. 2, pp. 284–286, Feb. 2003.

[14] W. Zhang, J. A. Williains, and I. Bennion, "Optical fiber delay line filter free of limitation imposed by optical coherence," *Elect. Lett.*, vol. 35, no. 24, pp. 2133–2134, Nov. 1999.

Mahmoud S. Rasras (M'05) received the Ph.D. degree in physics from the Catholic University of Leuven, Belgium, in 2000. His research on Spectroscopic Photon Emission Microscopy for CMOS-based semiconductor device reliability evaluation and testing was carried out at the Interuniversity Micro Electronics Center (IME).

In March 2001, he joined the Integrated Photonics Research Department at Bell Labs, Murray Hill, NJ, where he is designing components for next generation optical networks and government systems. He is currently the lead designer on a DARPA-funded project to demonstrate electronic and photonic integrated circuits (EPIC). He is also involved in research on an all-optical logic technology, where logical functions are realized in a hybrid silica/InP platform.

Kun-Yii Tu (M'04), photograph and biography not available at the time of publication.

Douglas M. Gill received the B.S. degree in physics from Buffalo State University, and the Masters and Ph.D. degrees from the University of Wisconsin–Madison, where he received the Newport Research Award for his graduate research.

He held a Research Associate position at Northwestern University, and is currently a Member of Technical Staff at Bell Labs of Alcatel-Lucent. His research interests include high-speed electrooptic transmitter design, the development of novel CMOS compatible electrooptic and thermooptic photonic components, and the application of advanced transmission formats for cost-effective data transmission.

Young-Kai Chen (F'98), photograph and biography not available at the time of publication.

Alice E. White (M'01–SM'09) received the B.A. degree in physics from Middlebury College and the M.A. and Ph.D. degrees in physics from Harvard University.

She is Vice President, Bell Labs North America, the largest R&D location of Alcatel-Lucent. She has a broad technical background in experimental solid-state physics and optics, including fabrication and implementation of optical fiber devices and integrated optical components for optical networks, semiconductor processing and devices, ion beam interactions with solids, and low temperature and vacuum techniques, with over 120 publications.

Dr. White is an active member of the American Physical Society (APS) and the Optical Society of America. She was elected Councilor-at-Large for the APS (1993) and was one of the founding members of the Forum on Industrial and Applied Physics (FIAP) of the APS. She is the recipient of the 1991 Maria Goeppert-Mayer Award from the APS and became a Fellow of the APS in 1995. More recently, she was recognized with the prestigious Bell Labs Fellow Award. She has served on the Advisory Board of NJIT's Murray Center for Women in Technology since 2004.

Sanjay S. Patel received the B.Tech. degree in chemical engineering from the Indian Institute of Technology, Kanpur, and the Ph.D. degree in chemical engineering and materials science from the University of Minnesota.

He is the Director of next-generation PON architectures in the Fixed Access Division at Alcatel-Lucent and a member of Bell Labs. He also serves as the Asia-Pacific Product Line Manager for the fiber-to-the-home product group. Prior to this, he was the Technical Manager for integrated photonics research at Bell Labs where he led a team that developed new ways of monolithically integrating optical components onto high-volume silicon platforms. His contributions at Bell Labs include the modeling of absorption of cell phone radiation in humans, self-assembly of 3-D photonic band gap structures, sol-gel manufacturing of optical fibers, modeling of polymer dynamics, and designing new materials for holographic storage.

Andrew Pomerene, photograph and biography not available at the time of publication.

Daniel Carothers, photograph and biography not available at the time of publication.

James Beattie, photograph and biography not available at the time of publication.

Mark Beals, photograph and biography not available at the time of publication.

Jurgen Michel, photograph and biography not available at the time of publication.

Lionel C. Kimerling, photograph and biography not available at the time of publication.